Advancements in Magnetic Nanoparticle Reconstruction Using Sequential Activation of Excitation Coil Arrays Using Magnetorelaxometry

Guillaume Crevecoeur[1], Daniel Baumgarten[2,3], Uwe Steinhoff[4], Jens Haueisen[2,3], Lutz Trahms[4], and Luc Dupré[1]

[1]Department of Electrical Energy, Systems and Automation, Ghent University, B-9000 Ghent, Belgium
[2]Institute of Biomedical Engineering and Informatics, Ilmenau University of Technology, Ilmenau, Germany
[3]Biomagnetic Center, University Hospital Jena, Jena, Germany
[4]Physikalisch-Technische Bundesanstalt, Berlin, Germany

Magnetic nanoparticles can be employed for a broad range of biomedical applications where the knowledge of the distribution of the magnetic nanoparticles is of importance for efficacy, patient's safety, etc. The need exists to have an as accurate as possible quantification of the unknown particles distribution. Magnetorelaxometry (MRX) measurements are able to measure the magnetic induction originating from a certain distribution of magnetically activated nanoparticles. Starting from these measurements it is possible to determine the distribution using a minimum norm estimation technique. This approach is however ill-posed. We sequentially activate the magnetic nanoparticles through the use of excitation coil arrays with the aim to reduce the ill-posedness. This paper presents some advancements in magnetic nanoparticle reconstruction in terms of reconstruction quality using numerical simulations. The results show that inhomogeneous sequential activation is a proper alternative to homogeneous activation with Helmholtz coils since an increase in accuracy with a factor ranging from 1.5 until 2 is obtained. The presented numerical techniques coupled to MRX measurements can be of significant aid so to have more quantitative knowledge of the biodistribution.

***Index Terms*—Accuracy, ill-posed inverse problem, magnetic nanoparticle, reconstruction.**

I. Introduction

SUPERPARAMAGNETIC iron oxide magnetic nanoparticles have a great potential for biological and medical applications, see e.g. [1]. Many issues still need to be adressed such as biocompatibility, toxicity, quantitative assessment of the distribution of the nanoparticles. The latter issue is of great importance for increasing the efficacy of the applications. Indeed, e.g. for the application of magnetic hyperthermia, the distribution needs to be known since different distributions of magnetic nanoparticles througout the tumour can lead to a different thermal response [2]. Other applications where a quantitative assessment is needed are magnetic drug targeting, tumor diagnosis, magnetic cell labelling; e.g. [3]–[5]. Magnetic nanoparticle imaging techniques were recently developed for qualitatively determining the distribution of the particles [6] and are based on the nonlinear magnetization response of the particles. The aim of this paper is to quantitatively reconstruct the magnetic nanoparticle concentration distribution using magnetorelaxometry. Magnetic nanoparticles can be activated using an external magnetic field where the single domains of the superparamagnetic nanoparticles are aligned with the local magnetic field. When switching off the external magnetic field, magnetic relaxation occurs following two different relaxation processes (Brown and Néel). The magnetic field originating from the particles in the different positions can be measured using superconducting quantum interference devices (SQUIDS) [7]. The magnetorelaxometry (MRX) measurements in the SQUIDS can be simulated through the use of a so-called forward model. On the other hand, when starting from the MRX measurements, it is possible to determine the spatial distribution of the magnetic nanoparticles by solving the corresponding inverse problem. This problem is however ill-posed since the number of unknowns is much higher than the number of measurement sites. In [8], MRX based reconstruction is applied using a minimum norm estimation technique, and in [9], temporal information is included in the inverse problem. The particles were homogeneously activated using Helmholtz coils.

A major problem in magnetic nanoparticle quantification remains the ill-posedness of the inverse problem. A possible solution is to include a priori information in the solution of the inverse problem. The methodology used here is to employ instead of homogeneous fields (Helmholtz coils), inhomogeneous fields (coil arrays) for the activation of the magnetic nanoparticles, as proposed in [10]. This paper defines a possible means of sequential activation using excitation coil arrays and compares numerically the reconstruction quality for homogeneous and inhomogeneous activation.

II. Activation of Magnetic Nanoparticles and MRX Measurements

A. Excitation Coil Array

We aim at reconstructing particles in a three-dimensional (3D) volume where the volume under study is discretized into N_{tot} voxels, each having volume V_v and where to each kth voxel a certain concentration $N_{P,k}$ $(k = 1, \ldots, N_{tot})$ is assigned to. The coordinate of the voxel is denoted by $\mathbf{r}_{P,k}$.

The amplitude of the magnetic moment of the nanoparticles in a certain voxel (with index k) as a function of the applied magnetic field $\mathbf{H}$ (with amplitude H), can be expressed through the Langevin function $(\mathcal{L})$: $m_k(H) = V_v N_{P,k} m \mathcal{L}(\mu_0 H m / k_B T)$ with m the magnetic moment of a nanoparticle, k_B the Boltzmann's constant, μ_0 the permeability of free air, and T the temperature. The

Manuscript received August 15, 2011; accepted October 15, 2011. Date of current version March 23, 2012. Corresponding author: G. Crevecoeur (e-mail: Guillaume.Crevecoeur@ugent.be).

Color versions of one or more of the figures in this paper are available online at http://ieeexplore.ieee.org.

Digital Object Identifier 10.1109/TMAG.2011.2173317

direction of $\mathbf{m}_k$ has the same direction as the magnetic field $\mathbf{H}$. Through a linear approximation of the Langevin function (i.e. truncation of Langevin's Taylor series after the linear term), the magnetic moment in a certain voxel can be calculated as

$$\mathbf{m}_k(\mathbf{r}_{P,k}) = \frac{V_v N_{P,k} m^2}{3k_B T}\mu_0 \mathbf{H}(\mathbf{r}_{P,k}) \quad (1)$$

Notice in (1) that the magnetic magnitude in the kth voxel is proportional to the magnetic particle concentration $N_{P,k}$ and that its orientation is in the direction of the locally applied magnetic field: $\mathbf{m}_k = a_{P,k}\mathbf{d}_{P,k}$ with amplitude $a_{P,k} = \|\mathbf{m}_k(\mathbf{r}_{P,k})\| \propto N_{P,k}$ and direction $\mathbf{d}_{P,k} = \mathbf{m}_k(\mathbf{r}_{P,k})/\|\mathbf{m}_k(\mathbf{r}_{P,k})\| = \mathbf{H}(\mathbf{r}_{P,k})/\|\mathbf{H}(\mathbf{r}_{P,k})\|$. We assume here that the fields generated by the magnetic dipoles do not affect $\mathbf{m}_k(\mathbf{r}_{P,k})$. By using a Helmholtz coils consisting of a pair of windings, as in [8], [9], $\mathbf{H}$ is approximately homogeneous in the central volume of the coil. However, when using coil arrays (with total of N_C coils), it becomes possible to 'control' the orientation $\mathbf{d}_{P,k}$ of the magnetic moments by the current $I_{C,i}$ $(i = 1, \ldots, N_C)$ flowing in each coil. Indeed, the magnetic field $\mathbf{H}_i(\mathbf{r}_{P,k})$ originating from a certain coil with current $I_{C,i}$ can be calculated using Biot-Savart's law.

B. Forward Problem: Simulation of the MRX Signals

A SQUID sensor (index j with $j = 1, \ldots, N_S$) at position $\mathbf{r}_{S,j}$ and predefined measurement axis $\mathbf{n}_{S,j}$, measures the magnetic induction of all magnetic dipoles: $B_j(\mathbf{r}_{S,j}) = \sum_{k=1}^{N_{tot}} b_k(\mathbf{r}_{S,j})$. The magnetic induction $b_k(\mathbf{r}_{S,j}) \equiv \mathbf{b}_k(\mathbf{r}_{S,j}) \cdot \mathbf{n}_{S,j}$ at sensor position $\mathbf{r}_{S,j}$ originating from a magnetic dipole at position $\mathbf{r}_{P,k}$ $(k = 1, \ldots, N_{tot})$ can then be calculated using

$$\frac{\mu_0}{4\pi}\left(\frac{3\mathbf{m}_k\cdot(\mathbf{r}_{S,j}-\mathbf{r}_{P,k})}{\|\mathbf{r}_{S,j}-\mathbf{r}_{P,k}\|^5}(\mathbf{r}_{S,j}-\mathbf{r}_{P,k}) - \frac{\mathbf{m}_k}{\|\mathbf{r}_{S,j}-\mathbf{r}_{P,k}\|^3}\right)\cdot\mathbf{n}_{S,j}. \quad (2)$$

The measured relaxation signal in MRX (i.e. $\Delta\mathbf{B} = \mathbf{B}_0 e^{-t_2/\tau} - \mathbf{B}_0 e^{-t_1/\tau}$ with $\mathbf{B}_0$ the induction when switching off the activation fields and known times t_1, t_2) is direct proportional to $\mathbf{B}_0$ with known relaxation constant τ. For simplification, we continue to use $\mathbf{B} = \mathbf{B}_0$ in the following and is a $N_S \times 1$-dimensional vector. All concentrations of the nanoparticles are grouped in the $N_P \times 1$-dimensional vector $\mathbf{a}_P$. In the static formulation, i.e. without adding the time dependence of the magnetic induction due to the relaxation, we have the following relation: $\mathbf{B} = \mathbf{L}\cdot\mathbf{a}_P$ with $\mathbf{L}$ being the $N_S \times N_P$-dimensional so-called lead field matrix that links the nanoparticle concentration at a certain position with the measurement site. Remark here that $\mathbf{n}_{S,j}$, the currents $I_{C,i}$ and the spatial information of coils, particles and SQUIDS, are enclosed within the lead field matrix $\mathbf{L}$ (see (2)).

C. Lead Field of Sequential Activation

The above lead field $\mathbf{L}$ can be extended when multiple sequential activations are performed. When defining N_A different activation sequences, then the measurement vector can be extended to a $N_S N_A \times 1$ vector by concatenating the measurement data (denoted as $\mathbf{B}_A$). The lead field matrix of all activations $(\mathbf{L}_A)$ becomes a $N_S N_A \times N_P$ matrix by concatenating the various lead fields. These lead fields can be computed by calculating the total magnetic field $\mathbf{H}(\mathbf{r}_{P,k}) = \sum_{i=1}^{N_C}\mathbf{H}_i(\mathbf{r}_{P,k})$ (and thus $\mathbf{d}_{P,k}$ in L_{jk} for a certain activation. In the case of sequential activation we have now: $\mathbf{B}_A = \mathbf{L}_A \cdot \mathbf{a}_P$. We group in the following the currents of a certain activation (index a) in a $N_C \times 1$ vector $\mathbf{I}_{C,a}$, $a = 1, \ldots, N_A$.

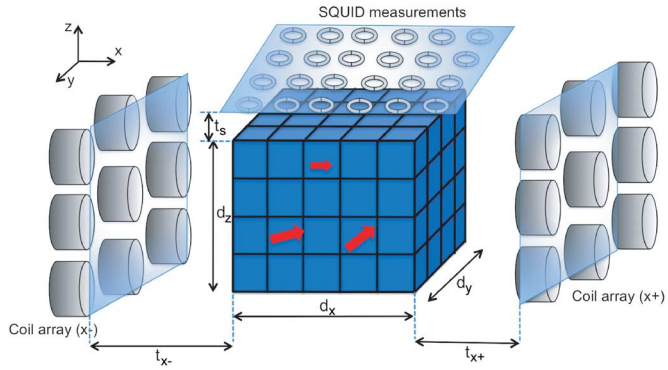

Fig. 1. Schematic representation of the coil arrays ($x-$ and $x+$), volume under study with N_{tot} discretizations, and the SQUID measurements. Due to the use of coil arrays that can be sequentially activated, the orientation of the particles $\mathbf{d}_{P,k}$ are not necessarily homogeneous.

III. Inverse Problem: Quantification of Magnetic Nanoparticle Distributions

A. Minimum Norm Estimation

The concentration of the magnetic nanoparticles can be recovered starting from measured SQUID signals $\mathbf{B}_{\text{meas}}$ using minimum norm estimation [11]. This estimation employs the truncated singular value decomposition method, which neglects singular values smaller than the parameter σ_r [12]:

$$\mathbf{a}_P^* = \mathbf{L}_{A,r}^{\dagger}\mathbf{B}_{\text{meas}} = (\mathbf{U}\Sigma\mathbf{V}^T)_r^{\dagger}\mathbf{B}_{\text{meas}} = \sum_{i=1}^{r}\frac{\mathbf{u}_i^T\mathbf{B}_{\text{meas}}}{\sigma_i}\mathbf{v}_i \quad (3)$$

with $\mathbf{u}_i$ and $\mathbf{v}_i$ the eigenvectors in respectively the $\mathbf{U}$ and $\mathbf{V}$ matrix. Σ is a diagonal matrix, whose diagonal elements are the singular values of matrix $\mathbf{L}_A = \mathbf{U}\Sigma\mathbf{V}^T$. The reconstructions in this paper are all computed in a 3D volume and we closely analyze the impact of sequential activation (with lead field $\mathbf{L}_A$) onto the recovery of the $\mathbf{a}_P^*$ distribution.

B. Simulation Setup

Fig. 1 represents the simulation setup used in this paper. In the case of homogeneous activation, a single coil is placed in the $x-$ plane and $x+$ plane. The figure represents the coil array where in each plane 9 coils are placed. Remark that coils were also placed in the $y-$ and $y+$ plane (not shown in figure for clarity) and coils in the $z-$ plane (i.e. plane parallel to the measurements plane but near the lower face of the volume under study). We placed here $N_C = 9 \times 5$ coils so to have a possible realistic implementation of sequential activation.

The geometrical constants defined in Fig. 1 are $d_x = d_y = d_z = 0.07$ m with a discretization of $16 \times 16 \times 16$ voxels. The distance of the coils to the volume under study is $t_{x-} = t_{x+} = 0.015$ m. If coils in the other plane are used, i.e. $(y-, y+, z-)$, then the same distance to volume under study is assumed. The measurements setup consists of $N_S = 97$ SQUID sensors with a first plane consisting of 81 sensors that are placed at a distance of $t_s = 8$ mm from the volume under study. The measurement angles of these sensors $\mathbf{n}_{S,j}$ $(j = 1, \ldots, 81)$ are in

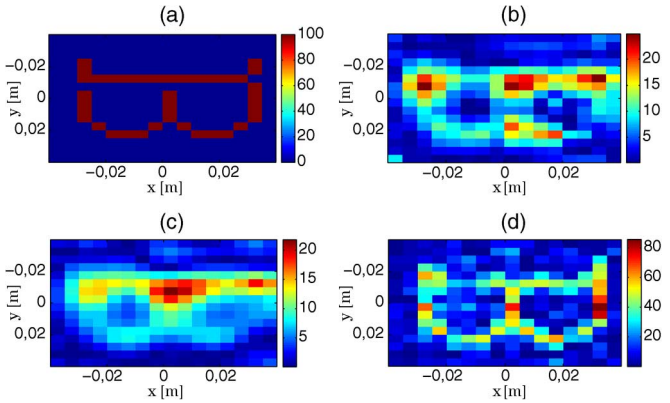

Fig. 2. (a) Actual magnetic nanoparticle concentration (p_2-plane), Reconstruction of particles with distance of p_2 from SQUIDS using (b) homogeneous field excitation, (c) sequential homogeneous activation, and (d) sequential inhomogeneous activation.

the z-direction and their locations $\mathbf{r}_{S,j}$ are within that plane on a regular grid with interdistance of 10 mm varying from -0.04 m until 0.04 m in the x and y direction. In a second plane with $t_s = 18$ mm, 16 SQUIDS are placed with $\mathbf{n}_{S,j}$ directions in the x and y direction. In the volume under study, magnetic nanoparticles are placed that need to be reconstructed. We placed three artificial B's (see Fig. 2(a)) in the xy-plane with a distance of $p_1 = 0.0127$ m, $p_2 = 0.0360$ m and $p_3 = 0.0780$ m from the closest SQUID measurement plane.

In the following, no real measurement data is included since the aim of this paper is to numerically establish whether the use of inhomogeneous sequential activation leads numerically to more accurate results. The forward data were computed with a volume discretization of 20^3 voxels in order to avoid making the inverse crime when solving the inverse problem for $N_{tot} = 16^3$ voxels. The correlation coefficient of the reconstructed concentration distribution compared to the actual concentration distribution is used to measure the reconstruction quality in all simulations. Another possible measure is to compare the decay of the singular values. Similarly as in [8], [9], the truncation index was chosen in such a way that the most accurate reconstruction was obtained. The value of $\sigma_r = 0.05$ was used in all presented simulations.

C. Defining the Sequential Activation

The sequential activation lead field $\mathbf{L}_A$ in (3) depends on the activation currents $\mathbf{I}_{C,a}$ $(a = 1, \ldots, N_A)$. In order to define these currents, we start from the spatial sensitivity of the kth particle: $S_k = \sum_{j=1}^{N_S} \|L_{jk}\|$. The L_{jk} (or S_k) values depend on the activation currents and is a measure of the impact of the kth particle upon the measurements. Fig. 3(a) shows the spatial sensitivity when the particles are activated using a Helmholtz coil (windings located here in the $x-$ and $x+$ plane). We can observe large sensitivity values for particles close to the coil and close to the sensor.

This sensitivity ($N_P \times 1$ vector $\mathbf{S}$) is function of $\mathbf{I}_C$:

$$\mathbf{S} = \mathbf{A} \cdot \mathbf{I}_C \tag{4}$$

with the $N_{tot} \times N_C$ interaction matrix $\mathbf{A}$. This matrix $\mathbf{A}$ needs to be calculated for $a_{P,k} = 1$ $(k = 1, \ldots, N_{tot})$ and depends on the geometry of the coils, sensors and particle locations.

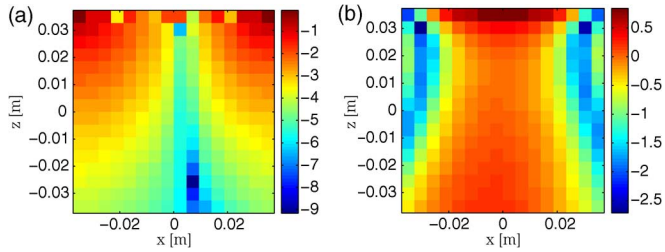

Fig. 3. Log-normal spatial sensitivity in the xz-plane for constant y near the middle when using (a) Helmholtz coil with windings in the $x-$ and $x+$ plane, (b) when using optimized current $\mathbf{I}_C^*$ in coil arrays.

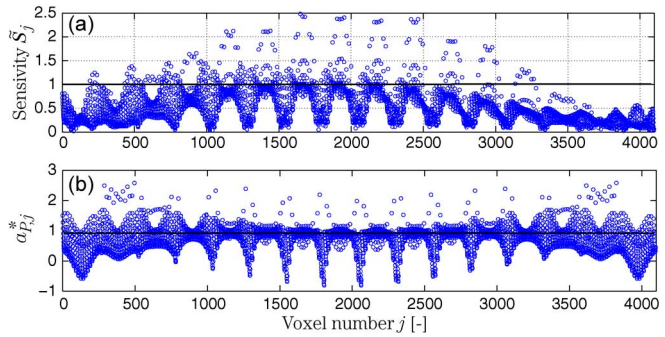

Fig. 4. (a) Calculated sensitivity $\mathbf{S}^*$ using activation with currents $\mathbf{I}_C^*$. (b) Recovered magnetic particle concentration $a_{P,j}^*$ when using the lead field with excitation $\mathbf{I}_C^*$.

The aim of inhomogeneous sequential activation is to achieve a more homogeneous spatial sensitivity so that particles located relatively far from the sensors and coils have more impact upon the measurements and thus on the inversion. In this way, the whole volume under study will have less preferred regions of accuracy, i.e. also regions located far from the sensors and coils will be more accurately reconstructed. In order to obtain this, we aim at $\mathbf{S}^* = \mathbf{1}$ (i.e. $S_k^* = 1$ for all voxels) or

$$\mathbf{I}_C^* = \mathbf{A}^\dagger \cdot \mathbf{1} \tag{5}$$

Since (4) is an overdetermined system of equations, the sensitivity $\mathbf{S}^* = \mathbf{A} \cdot \mathbf{I}_C^*$ will not equal $\mathbf{1}$. This can be observed in Fig. 3(b) and Fig. 4(a). However, the sensivity is increased for particles located relatively far from the sensors. This is achieved by means of the activation of coils located in the $z-$plane and the coils located far from the sensors. In order to show that the reconstruction quality depends on the sensitivity, we solve the inverse problem (3) with $\mathbf{B}_{\text{meas}} = \mathbf{L} \cdot \mathbf{1}$ and $\mathbf{L}_A$ the lead field corresponding with $\mathbf{I}_C^*$. Fig. 4(b) shows that the accuracy of the reconstructed concentrations $a_{P,j}^*$ which should be 1, correlate well with the sensitivity values corresponding with $\mathbf{I}_C^*$, i.e. low sensitivity values give large discrepancy errors.

Starting from $\mathbf{S}^*$, we determine the next activations. We 'target' the particles that have a low sensitivity in $\mathbf{S}^*$. We implemented the following procedure for determining the N_a sequential activations. Let us define a threshold $\alpha = 1/Na$ where the wanted sensitivity of the ath activation $S_j^{(a)}$ is 1 if $\alpha(a-1) < S_j^* < \alpha a$ (otherwise 0) with a the index of the activation $(a = 1, \ldots, N_a)$. Similar to (5), it is then possible to determine the activation currents $\mathbf{I}_{C,a}$. Note that in each sequential activation, a selective sensitivity is used.

Fig. 5 shows that the enforced currents can rise very high because the system of equations is overdetermined and because we

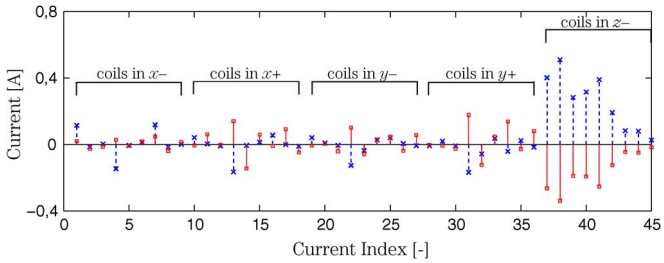

Fig. 5. Enforced currents in the first (-x-) and second activation (-o-).

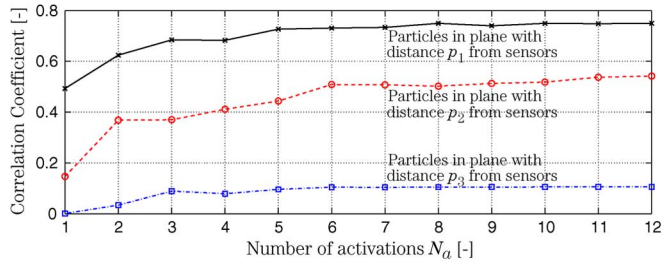

Fig. 6. Correlation coefficients of the assumed concentration distribution compared to the reconstructed concentration for increasing number of activations. The correlation coefficients are calculated within the planes that are at a distance p_1, p_2 and p_3 from the SQUIDS.

are working in a linear approximation of the Langevin function (1). Indeed, higher currents lead to a higher amplitude of $\mathbf{m}_k$ and thus a larger lead field contribution. Simulations were carried out for coils with 10 windings. Further research is needed for making this 'optimization of activation current' more realistic, non-linear and with constraints with respect to the limits of the SQUIDS. Also, the excitation system (number of windings, diameter of windings, number of coils, etc.) itself can be optimized, taking into account the feasibility of the system, e.g., in terms of power loss of excitation coils.

D. Sequential Activation

In a first stage, we recovered magnetic nanoparticles that are activated by a Helmholtz coil (with windings at $t_{x-} = t_{x+} = 0.015$ m). This Helmholtz coil yields an approximate homogeneous magnetic field $\mathbf{H}(\mathbf{r}_{P,k})$ in the volume under study and thus a $\mathbf{d}_{P,k} = \mathbf{1}_x$ for all N_{tot} voxels. Fig. 2(b) shows the reconstruction results for particles located in the p_2 plane. In a second stage, we sequentially activated two Helmholtz coils with a pair of windings at $(x-, x+)$ and a pair of windings at $(y-, y+)$ yielding in the first activation the same lead field as in previous stage with $\mathbf{d}_{P,k} = \mathbf{1}_x$, and in the second activation homogeneous $\mathbf{d}_{P,k} = \mathbf{1}_y$ directions for all voxels. This resulted in a distribution depicted in Fig. 2(c). Finally, we employed the coil arrays using the approaches presented in Section III-C for $N_A = 4$. Fig. 2(d) shows that the reconstructed distributions are quantitatively closer to the original distribution compared to the previous approaches. Fig. 6 illustrates more quantitatively the increase in accuracy (correlation of the recovered distribution with the original distribution) when increasing the number of activations N_a. We observe that the rate of increase is higher for the magnetic particles located at distance p_2 from the sensors when using sequential activation. Sequential activation with inhomogeneous fields can yield an increase of the correlation, compared with the actual distribution, with a factor ranging from 1.5 until 2. It is clear from Fig. 6 that the accuracy of the recovered particles in the plane located far away from the sensors (p_3), is poor even with sequential activation. The reason for this is that the particles are located too far from the sensor, and/or that the sequence defined in Section III-C is suboptimal and/or that more than 9 coils should be used in the coil array. More research is needed for optimally activating the particles and what activation hardware is needed in order to make more advancements in quantitative magnetic nanoparticle reconstructions.

IV. Conclusions

This paper proposes some advancements in magnetic nanoparticle reconstruction using sequential activation of excitation coil arrays. We compared results when using homogeneous activation, sequential homogeneous activation and sequential inhomogeneous activation. We observed that it is key to attain an as high as possible sensitivity of the particles to the sensors. In order to obtain this, it is possible to optimize the excitation current through the coil arrays by using the interaction between every coil and the sensors. We observed that sequential activation results in a better quality of reconstruction, especially for particles located relatively far away from the sensors. It is clear that the methodologies presented in this paper are a first step for sequential activation in the framework of inverse magnetic nanoparticle reconstruction and that some more advancements are possible and needed.

Acknowledgment

G. Crevecoeur is a postdoctoral researcher of the FWO. This work was carried out during a long visit of G. Crevecoeur, funded by the FWO, at the Ilmenau University of Technology.

References

[1] Q. A. Pankhurst *et al.*, "Applications of magnetic nanoparticles in biomedicine," *J. Phys. D: Appl. Phys.*, vol. 36, pp. R167–R181, 2003.
[2] P. Moroz, S. K. Jones, and B. N. Gray, "Tumor response to arterial embolization hyperthermia and direct injection hyperthermia in a rabbit liver tumor model," *J. Surgical Oncol.*, vol. 80, p. 14956, 2002.
[3] N. G. Portney and M. Ozcan, "Nano-oncology: Drug delivery, imaging, and sensing," *Anal. Bioanal. Chem.*, vol. 384, pp. 620–630, 2006.
[4] Q. A. Pankhurst *et al.*, "Progress in applications of magnetic nanoparticles in biomedicine," *J. Phys. D: Appl. Phys.*, vol. 42, no. 22, p. 224001, 2009.
[5] T. Neuberger *et al.*, "Superparamagnetic nanoparticles for biomedical applications: Possibilities and limitations of a new drug delivery system," *J. Magn. Magn. Mat.*, vol. 293, pp. 483–496, 2005.
[6] B. Gleich and J. Weiszenecker, "Tomographic imaging using the nonlinear response of magnetic particles," *Nature*, vol. 435, pp. 1214–1217, 2005.
[7] E. R. Flynn and H. C. Bryant, "A biomagnetic system for ==*in vivo* cancer imaging," *Phys. Med. Biol.*, vol. 50, pp. 1273–1293, 2005.
[8] D. Baumgarten *et al.*, "Magnetic nanoparticle imaging by means of minimum norm estimates from remanence measurements," *Med. Biol. Eng. Comput.*, vol. 46, pp. 1177–1185, 2008.
[9] D. Baumgarten and J. Haueisen, "A spatio-temporal approach for the solution of the inverse problem in the reconstruction of magnetic nanoparticle distributions," *IEEE Trans. Magn.*, vol. 46, no. 8, pp. 3496–3499, 2010.
[10] U. Steinhoff *et al., Biomed. Tech.*, vol. 55, no. S1, pt. A, pp. 22–25, 2010.
[11] J. Wang, S. Williamson, and L. Kaufman, "Magnetic source images determined by a lead-field analysis: The unique minimum-norm least squares estimation," *IEEE Trans. Biomed. Eng.*, vol. 39, pp. 665–675, 1992.
[12] P. C. Hansen, "The truncated SVD as a method for regularization," *BIT*, vol. 27, p. 534553, 1987.